

Calculation of steady-state distributions of concentrations and potential controlled by diffusion and migration of ions

A. KATAGIRI

College of Liberal Arts, Kyoto University, Sakyo-ku, Kyoto 606, Japan

Received 23 March 1990; revised 5 October 1990

A numerical method is proposed for the calculation of concentration, potential, and current distributions in electrochemical cells controlled by diffusion and migration of ions. Thus a hypothetical variable $v(x, y, t)$ is assumed to satisfy a differential equation which is similar to that of non-steady-state heat conduction and corresponds, at steady state, to Poisson's equation for the potential. The differential equation for $v(x, y, t)$ and the diffusion-migration equations of ions are simultaneously solved by a finite difference method. Examples of calculation are given for single and mixed electrolyte solutions in one- and two-dimensional cells. The proposed method is applicable to systems in which bipolarity occurs.

Nomenclature

a	interelectrode distance	z_i	charge number of species i
c_i	concentration of species i	α	hypothetical constant (compared to thermal diffusivity)
C_i	dimensionless concentration of species i (c_i/c_{M0})	α_c	transfer coefficient
D_i	diffusion coefficient of species i	β	dimensionless parameter ($F^2 a^2 c_{M0}/\epsilon RT$)
F	Faraday constant	γ	dimensionless parameter ($F^2 c_{M0} a^3/K_B RT$)
i	current density	ϵ	dielectric constant
I	dimensionless current density ($ia/FD_M c_{M0}$)	Θ	dimensionless time ($D_M t/a^2$)
j_i	flux of species i	σ	dimensionless area (S/a^2)
J_i	dimensionless flux of species i ($j_i a/D_M c_{M0}$)	$\phi(x, y)$	potential of solution
K_B	hypothetical constant of bipolar metal (compared to heat capacity)	ϕ_M	potential of metal
n	distance from surface	$\Phi(X, Y)$	dimensionless potential of solution ($F\phi(x, y)/RT$)
N	dimensionless distance from surface	Φ_M	dimensionless potential of metal ($F\phi_M/RT$)
R	gas constant	$\Psi(X, Y)$	stream function defined by Equation 28
S	surface area	∇	vector operator ($\frac{\partial}{\partial x}, \frac{\partial}{\partial y}$)
t	time		
T	absolute temperature		
$v(x, y, t)$	hypothetical variable which, for $t = \infty$, corresponds to $\phi(x, y)$		
$V(X, Y, \Theta)$	dimensionless variable ($Fv(x, y, t)/RT$) which, for $\Theta = \infty$, corresponds to $\Phi(X, Y)$		
x, y	Cartesian coordinates		
X, Y	dimensionless Cartesian coordinates ($x/a, y/a$)		
			*Boldface letters indicate vector quantities.
		<i>Subscripts</i>	
		A	anion A ⁻
		B	bipolar metal
		i	species i
		M	metal M or cation M ⁺
		S	cation S ⁺
		0	initial or standard state

1. Introduction

Calculation of potential and current distributions in electrochemical cells has been an important subject in electrochemical engineering [1-4]. Much work has

been reported for the case in which the concentration gradients of ions in the solution can be neglected, where Laplace's equation for the potential holds [5-13]. Even when mass transport affects the current distribution, Laplace's equation is often satisfied in

the bulk solution since the concentration variation is restricted to a thin diffusion layer at the electrode [14, 15]. However, when a large current flows in an electrolytic cell or a battery, nonuniform distributions of concentrations may developed throughout the cell. Nonuniformity of ionic concentrations may also become significant in a galvanic cell associated with local corrosion of metal such as pitting and crevice corrosion. In such cases Laplace's equation for the potential is no longer valid. If we consider cases in which mass transfer occurs only by diffusion and migration, concentration and potential distributions are governed by relevant diffusion-migration equations for ions and Poisson's equation for the potential (or the electroneutrality condition as an approximation of Poisson's equation). In the one-dimensional case, such problems have been solved using the total current as an independent variable. Thus, analytical solutions have been obtained using the electroneutrality condition [16, 17], and numerical calculation has been reported using Poisson's equation [18]. In two- and three-dimensional cases, the problem is far more difficult to solve since the current density is a vector variable. A two-dimensional model has been proposed which takes into account the diffusion, migration, and unsteady-state effects in a solution of single electrolyte [19]. However, the situation is complicated if the solution contains multiple electrolytes of comparable concentrations, and if boundary conditions are not simple as in the case of a bipolar electrode.

In previous papers the potential and current distributions at a bipolar electrode have been considered [20, 21], and a numerical method has been proposed for the calculation of potential distribution using an analogy with heat conduction [22, 23]. The present paper shows that a similar method is applicable to the calculation of concentration and potential distributions controlled by diffusion and migration of ions. Such a situation may be encountered in a cell in which the solution is stagnant or held in a matrix. The proposed method is particularly useful when bipolarity occurs in the cell. Only one- and two-dimensional distributions are considered here, although there is no substantial limitation to the three-dimensional calculation.

2. Principle

The assumptions employed are: (a) that the electrolyte solution is dilute and ideal; (b) that convection and homogeneous chemical reactions do not occur; and (c) that electroneutrality is valid in the solution except for the double layer region. Then the flux of species i in the bulk of the solution is expressed as

$$j_i = -\frac{z_i F D_i c_i}{RT} \nabla \phi - D_i \nabla c_i \quad (1)$$

where c_i is the concentration of species i , z_i is the charge number, D_i is the diffusion coefficient, F is Faraday's constant, R is the gas constant, T is the absolute temperature, and ϕ is the electric potential in

the solution. The rate of change of concentration c_i is obtained from mass balance of species i :

$$\frac{\partial c_i}{\partial t} = -\nabla \cdot j_i = \frac{z_i F}{RT} \nabla(D_i c_i \nabla \phi) + \nabla(D_i \nabla c_i) \quad (2)$$

At steady state,

$$\frac{z_i F}{RT} \nabla(D_i c_i \nabla \phi) + \nabla(D_i \nabla c_i) = 0 \quad (3)$$

The electroneutrality condition is

$$\sum_i z_i c_i = 0 \quad (4)$$

In principle, Equations 3 and 4 govern the steady-state distributions of c_i and ϕ . However, it is not easy to solve these equations except for the one-dimensional case (see Appendix). If, in particular, a bipolar electrode is involved, even numerical calculation will be difficult since boundary values of concentrations and potential at the bipolar electrode cannot be specified in advance.

Now, let us consider Poisson's equation for ϕ instead of the electroneutrality condition (Equation 4).

$$\nabla^2 \phi = -\frac{F}{\varepsilon} \sum_i z_i c_i \quad (5)$$

Here ε is the dielectric constant of the solution. For pure water at 25°C, $\varepsilon = 78.3 \times 8.854 \times 10^{-12} \text{ C}^2 \text{ J}^{-2} \text{ m}^{-1} = 6.93 \times 10^{-12} \text{ CV}^{-1} \text{ cm}^{-1}$. The numerical value of F/ε is so large ($1.392 \times 10^{16} \text{ V cm equiv}^{-1}$ for pure water) that Equation 5 does not necessarily reduce to Laplace's equation although electroneutrality is a very good approximation. In principle Equation 2 (or Equation 3 at steady state) and Equation 5 determine the distributions of c_i and ϕ , but solving these equations is difficult except for some simple cases.

There is a similarity between the potential distribution in a solution and the temperature distribution in a heat-conducting medium [24]. Thus the potential distribution which obeys Poisson's equation can be compared to the steady-state distribution of temperature with heat generation. Now, let us assume a hypothetical variable $v(x, y, t)$ and a differential equation

$$\frac{\partial v}{\partial t} = \alpha \left\{ \nabla^2 v + \frac{F}{\varepsilon} \sum_i z_i c_i \right\} \quad (6)$$

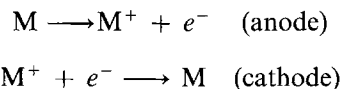
which is similar to the equation of non-steady-state heat conduction. Here, α is a hypothetical constant (compared to the thermal diffusivity in heat conduction problems). When $\partial v/\partial t = 0$ for $t = \infty$, Equation 6 has a form identical to Equation 5, and the value of $v(x, y, \infty)$ corresponds to the potential $\phi(x, y)$. Therefore, if we solve Equation 6 simultaneously with Equation 2, in which $\phi(x, y)$ is replaced by $v(x, y, t)$, and obtain a steady-state ($\partial v/\partial t = \partial c_i/\partial t = 0$ for $t = \infty$), the values of $v(x, y, \infty)$ and $c_i(x, y, \infty)$ are regarded as the solutions of Equations 3 and 5. It should be mentioned, however, that the variable $v(x, y, t)$ has the meaning of potential only when $\partial v/\partial t$ converges to zero.

The current density is then given by

$$i = F \sum_i z_i j_i = - \frac{F^2}{RT} \left(\sum_i z_i^2 D_i c_i \right) \nabla \phi - F \sum_i (z_i D_i \nabla c_i) \quad (7)$$

3. Numerical calculation procedure

Let us consider a cell containing a mixed solution of two 1:1 electrolytes, M^+A^- and S^+A^- , where the anodic and cathodic reactions are the dissolution and deposition of metal M:



Thus S^+A^- represents a supporting electrolyte. As is usually the case, the thickness of the double layer at the electrodes and at the insulating walls is assumed to be negligibly small compared to the interelectrode distance and the electrode width. Then the boundary of the bulk solution, which is the solution side limit of the electric double layer, can be approximately taken at the surfaces of electrodes and insulating walls [25]. Therefore, boundary conditions at the anode and cathode and at insulating walls are formulated as follows. Since the fluxes of non-electroactive species S^+ and A^- in the normal direction to the surface are zero,

$$\frac{FD_S}{RT} c_S \frac{\partial \phi}{\partial n} + D_S \frac{\partial c_S}{\partial n} = 0 \quad (8)$$

$$- \frac{FD_A}{RT} c_A \frac{\partial \phi}{\partial n} + D_A \frac{\partial c_A}{\partial n} = 0 \quad (9)$$

where n is the distance from the surface. Using Equations 7, 8, and 9, the current density in the normal direction at the electrode surface is expressed as

$$i = - \frac{F^2 D_M}{RT} c_M \frac{\partial \phi}{\partial n} - F D_M \frac{\partial c_M}{\partial n} \quad (10)$$

The current density is a function of the potential difference between the electrode and the nearby solution and of the concentration c_M :

$$i = f\{(\phi_M - \phi), c_M\} \quad (11)$$

Therefore, the third boundary condition is given as

$$\frac{F^2 D_M}{RT} c_M \frac{\partial \phi}{\partial n} + F D_M \frac{\partial c_M}{\partial n} = - f\{(\phi_M - \phi), c_M\} \quad (12)$$

In the one-dimensional case, the condition of constant flux of M^+ may be used instead of Equation 12. Since electroneutrality is assumed in the bulk solution, the fourth boundary condition is

$$c_M + c_S - c_A = 0 \quad (13)$$

Boundary conditions at insulating walls are given from zero fluxes of all species (M^+ , S^+ , and A^-) and from the electroneutrality condition.

Assuming that the anode and the cathode are paral-

lel plates positioned at the distance a , it is convenient to use the following dimensionless quantities: $X = x/a$, $Y = y/a$, $N = n/a$, $\Theta = D_M t/a^2$, $C_i = c_i/c_{M0}$, $\Phi = F\phi/RT$, $V(X, Y, \Theta) = Fv(x, y, t)/RT$, $I = ia/FD_M c_{M0}$, where c_{M0} is the initial concentration of M^+ as the reference species. Then Equation 2 (for M^+ , S^+ , and A^-) and Equation 6 are rewritten in the following dimensionless forms.

$$\frac{\partial C_M}{\partial \Theta} = \frac{\partial}{\partial X} \left(C_M \frac{\partial V}{\partial X} \right) + \frac{\partial}{\partial Y} \left(C_M \frac{\partial V}{\partial Y} \right) + \frac{\partial^2 C_M}{\partial X^2} + \frac{\partial^2 C_M}{\partial Y^2} \quad (14)$$

$$\frac{\partial C_S}{\partial \Theta} = \frac{D_S}{D_M} \left\{ \frac{\partial}{\partial X} \left(C_S \frac{\partial V}{\partial X} \right) + \frac{\partial}{\partial Y} \left(C_S \frac{\partial V}{\partial Y} \right) + \frac{\partial^2 C_S}{\partial X^2} + \frac{\partial^2 C_S}{\partial Y^2} \right\} \quad (15)$$

$$\frac{\partial C_A}{\partial \Theta} = \frac{D_A}{D_M} \left\{ - \frac{\partial}{\partial X} \left(C_A \frac{\partial V}{\partial X} \right) - \frac{\partial}{\partial Y} \left(C_A \frac{\partial V}{\partial Y} \right) + \frac{\partial^2 C_A}{\partial X^2} + \frac{\partial^2 C_A}{\partial Y^2} \right\} \quad (16)$$

$$\frac{\partial V}{\partial \Theta} = \frac{\alpha}{D_M} \left(\frac{\partial^2 V}{\partial X^2} + \frac{\partial^2 V}{\partial Y^2} \right) + \frac{\alpha \beta}{D_M} (C_M + C_S - C_A) \quad (17)$$

where β is a dimensionless parameter $F^2 a^2 c_{M0}/\epsilon RT$ and has a typical value of 5.42×10^{14} for $a = 1$ cm, $c_{M0} = 10^{-3}$ mol cm $^{-3}$, $\epsilon = 6.93 \times 10^{-12}$ CV $^{-1}$ cm $^{-1}$, and $T = 298$ K. Boundary conditions corresponding to Equations 8, 9, 12 and 13 are as follows.

$$C_S \frac{\partial V}{\partial N} + \frac{\partial C_S}{\partial N} = 0 \quad (18)$$

$$- C_A \frac{\partial V}{\partial N} + \frac{\partial C_A}{\partial N} = 0 \quad (19)$$

$$C_M \frac{\partial V}{\partial N} + \frac{\partial C_M}{\partial N} = - f\{(V_M - V), C_M\} \quad (20)$$

$$C_M + C_S - C_A = 0 \quad (21)$$

Boundary conditions at the insulating walls are similarly written in dimensionless forms.

For finite difference calculations we can use forward difference approximations for derivatives with respect to Θ and central difference approximations for derivatives with respect to X and Y as exemplified by

$$\frac{\partial C_M}{\partial \Theta} = \frac{(C_M)_{i,j,k+1} - (C_M)_{i,j,k}}{\Delta \Theta}$$

$$\frac{\partial C_M}{\partial X} = \frac{(C_M)_{i+1,j,k} - (C_M)_{i-1,j,k}}{2\Delta X}$$

$$\frac{\partial^2 C_M}{\partial X^2} = \frac{(C_M)_{i+1,j,k} - 2(C_M)_{i,j,k} + (C_M)_{i-1,j,k}}{(\Delta X)^2}$$

where ΔX , ΔY , and $\Delta \Theta$ are finite differences of X , Y , and Θ , and i , j , and k are the ordinal numbers corre-

sponding to X , Y , and Θ , respectively:

$$X = i\Delta X, \quad Y = j\Delta Y, \quad \Theta = k\Delta\Theta$$

Then we obtain a set of difference equations which allow calculation of explicit values of the C_M , C_S , C_A , and V at the time step $k + 1$ from the C_M , C_S , C_A , and V values at the time step k . Starting from appropriate initial conditions we can continue such calculations until a steady state is reached.

Convergence to a steady state was attained by using appropriate values of ΔX , ΔY , $\Delta\Theta$, and $\alpha\beta/D_M$. Typical values used were $\Delta\Theta = 0.001$, $\Delta X = \Delta Y = 0.05$, and $\alpha\beta/D_M = 100$. The time required for convergence on a personal computer was several tens of minutes to several hours. The terms $(\alpha/D_M)(\partial^2 V/\partial X^2 + \partial^2 V/\partial Y^2)$ in Equation 17 was insignificant since α/D_M was very small: $\alpha/D_M = 1.85 \times 10^{-13}$ for $\beta = 5.42 \times 10^{14}$. Therefore, $\partial V/\partial\Theta = 0$ in Equation 17 implies the electroneutrality condition.

4. Results of calculation

The proposed method was tested in the simple one-dimensional case in which an analytical method was applicable. Thus it was assumed that a solution of single 1:1 electrolyte M^+A^- was electrolyzed with parallel plate electrodes of infinite size. The diffusion coefficients D_M and D_A were taken to be equal. Figure 1 shows the potential distribution and concentration distributions of M^+ and A^- calculated for $I = -2$ (half the limiting current density; see Appendix). Concentrations of M^+ and A^- are almost equal at every point in accordance with the electroneutrality condition. However, Laplace's equation for the potential is not satisfied as apparent from non-linearity of the potential gradient. The solid lines in

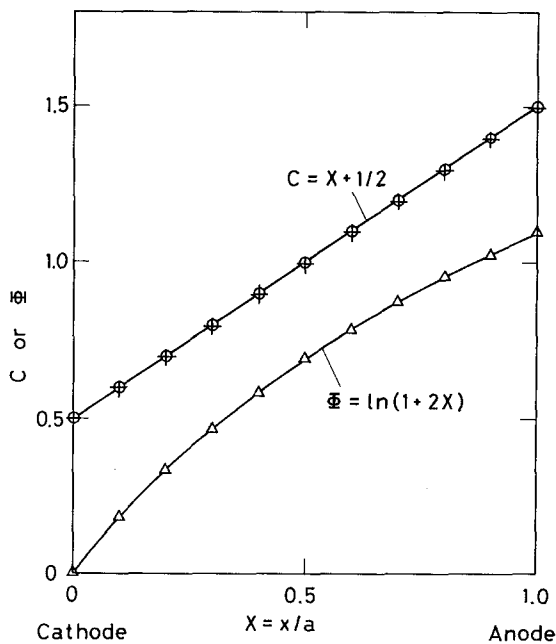


Fig. 1. One-dimensional distributions of concentrations and potential in a solution of single electrolyte (M^+A^-). Current density, $i = -2FD_M c_0/a$ ($I = -2$); (O) $C_M (=c_M/c_0)$; (+) $C_A (=c_A/c_0)$; (Δ) $\Phi (=F\phi/RT)$.

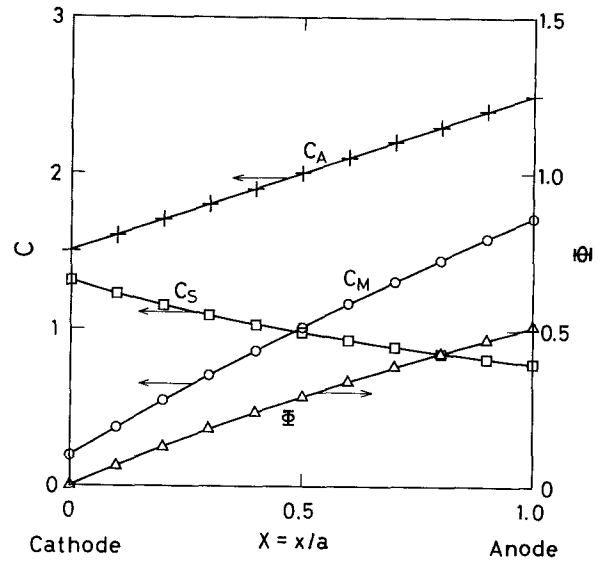


Fig. 2. One-dimensional distributions of concentrations and potential in a solution of mixed electrolytes ($M^+A^- + S^+A^-$). Current density, $i = -2FD_M c_{M0}/a$ ($I = -2$); (O) $C_M (=c_M/c_{M0})$; (\square) $C_S (=c_S/c_{M0})$; (+) $C_A (=c_A/c_{M0})$; (Δ) $\Phi (=F\phi/RT)$.

Fig. 1 represent the following equations obtained by analytical calculation (see Appendix):

$$C_M = C_A = X + \frac{1}{2} \quad (22)$$

$$\Phi = \ln(1 + 2X) \quad (23)$$

Good agreement is seen between numerical and analytical calculations.

One-dimensional distributions of concentrations and potential were also calculated for a solution containing two electrolytes M^+A^- and S^+A^- . Calculation was performed in the case where concentrations of M^+A^- and S^+A^- were equal ($C_{S0} = 1$, $C_{A0} = 2$), and the current density was $I = -2$. The diffusion coefficients D_M , D_S , and D_A were taken to be equal. Figure 2 shows the calculated distributions of C_M , C_S , C_A , and Φ . The solid lines represent the following equations obtained by the analytical calculation (see Appendix):

$$C_A = X + \frac{3}{2} \quad (24)$$

$$C_S = \frac{1}{(X + 3/2) \ln(5/3)} \quad (25)$$

$$C_M = X + \frac{3}{2} - \frac{1}{(X + 3/2) \ln(5/3)} \quad (26)$$

$$\Phi = \ln\left(1 + \frac{2X}{3}\right) \quad (27)$$

Again, good agreement is seen between the numerical and analytical calculations.

Next, two-dimensional distributions were considered in a solution of single electrolyte M^+A^- in the rectangular cell, shown in Fig. 3, with the geometry of $a:c = 1:1$ and $b:c = 1:2$. It was assumed that there was no overpotential at both electrodes: constant potentials were assigned to the electrolyte at the electrode surface. Only a half of the cell was considered. Figure 4 shows contours of the M^+ concentration

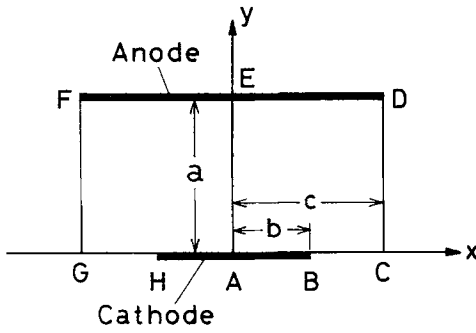


Fig. 3. Two-dimensional model of a rectangular cell. $a/c = 1$; $b/c = 1/2$.

which was almost exactly equal to the A^- concentration at any point. This is the electroneutrality condition which is anticipated in the bulk solution. Figure 4b shows the potential and current distributions (equipotential lines and current lines). The current lines were drawn as contours of the stream function which was calculated by

$$\Psi(X, Y) = \Psi(X_0, Y_0) - \int_{X_0}^X I_y(X, Y_0) dX + \int_{Y_0}^Y I_x(X, Y) dY \quad (28)$$

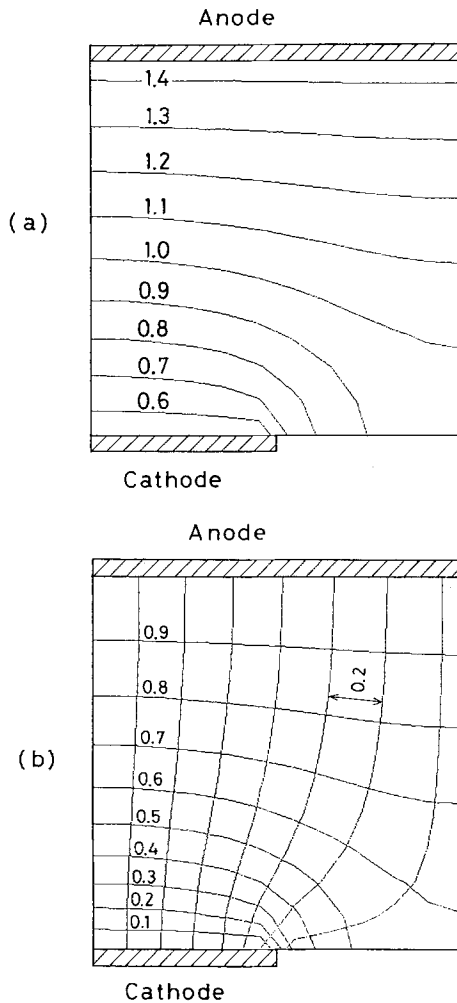


Fig. 4. (a) Concentration distribution of $M^+(A^-)$ and (b) potential and current distributions in a solution of single electrolyte (M^+A^-). $\Phi(Y = 0) = 0$; $\Phi(Y = 1) = 1$. In (a) the numbers indicate the value of $C_M (\sim C_A)$; in (b) the lines with numbers are equipotential lines, each number indicating the value of Φ . The separation between adjacent current lines corresponds to $\Delta\Psi = 0.2$.

where $I_x(X, Y)$ and $I_y(X, Y)$ are dimensionless forms of the x - and y -component of the current density. In the present case $I_x(X, Y)$ and $I_y(X, Y)$ are expressed as

$$I_x(X, Y) = - \left(C_M \frac{\partial\Phi}{\partial X} + \frac{\partial C_M}{\partial X} \right) \quad (29)$$

$$I_y(X, Y) = - \left(C_M \frac{\partial\Phi}{\partial Y} + \frac{\partial C_M}{\partial Y} \right) \quad (30)$$

It is noted in Fig. 4b that the ratio of the separation between adjacent potential lines to the separation between adjacent current lines varies from place to place. This is an indication that the local potential gradient is not proportional to the local current density, that is, Ohm's law does not hold.

Two-dimensional distributions of concentrations, potential, and current were also calculated for a mixed solution of two electrolytes $M^+A^- + S^+A^-$ under similar conditions as in the case of one-dimensional calculation. Figure 5a, b, and c shows the obtained distributions of the M^+ , S^+ , and A^- concentrations, respectively. The sum of C_M and C_S coincides with C_A at every point. It is noted that the supporting electrolyte S^+A^- is enriched near the cathode. Figure 5d shows the corresponding potential and current distributions. The present method is applicable to electrolyte systems with any number of ionic species.

We can take into account electrode kinetics, for example, of the Butler-Volmer type:

$$i = i_0 \left[\exp \left(\frac{(1 - \alpha_c)F(\phi_M - \phi)}{RT} \right) - \frac{c_M}{c_{M0}} \exp \left(\frac{-\alpha_c F(\phi_M - \phi)}{RT} \right) \right] \quad (31)$$

Boundary conditions at the electrode surface are rather complicated. Assuming a simple M^+A^- solutions ($c_S = 0$ and $c_M = c_A$), dimensionless forms of boundary conditions (Equations 19, 20, and 21) are now written:

$$-C_A \frac{\partial V}{\partial N} + \frac{\partial C_A}{\partial N} = 0 \quad (32)$$

$$C_M \frac{\partial V}{\partial N} + \frac{\partial C_M}{\partial N} = -I_0 \left\{ \exp \{ (1 - \alpha_c)(V_M - V) \} - C_M \exp \{ -\alpha_c(V_M - V) \} \right\} \quad (33)$$

$$C_M - C_A = 0 \quad (34)$$

where $V_M = Fv_M/RT$ and $I_0 = i_0 a/FD_M c_{M0}$. Equations 32 to 34 determine the C and V values at the electrode surface. For the cathode, for example (see Fig. 3), the corresponding difference expressions are

$$- \left(\frac{(C_A)_{i,1,k} + (C)_{i,0,k}}{2} \right) \left(\frac{(V)_{i,1,k} - (V)_{i,0,k}}{\Delta Y} \right) + \left(\frac{(C_A)_{i,1,k} - (C)_{i,0,k}}{\Delta Y} \right) = 0 \quad (35)$$

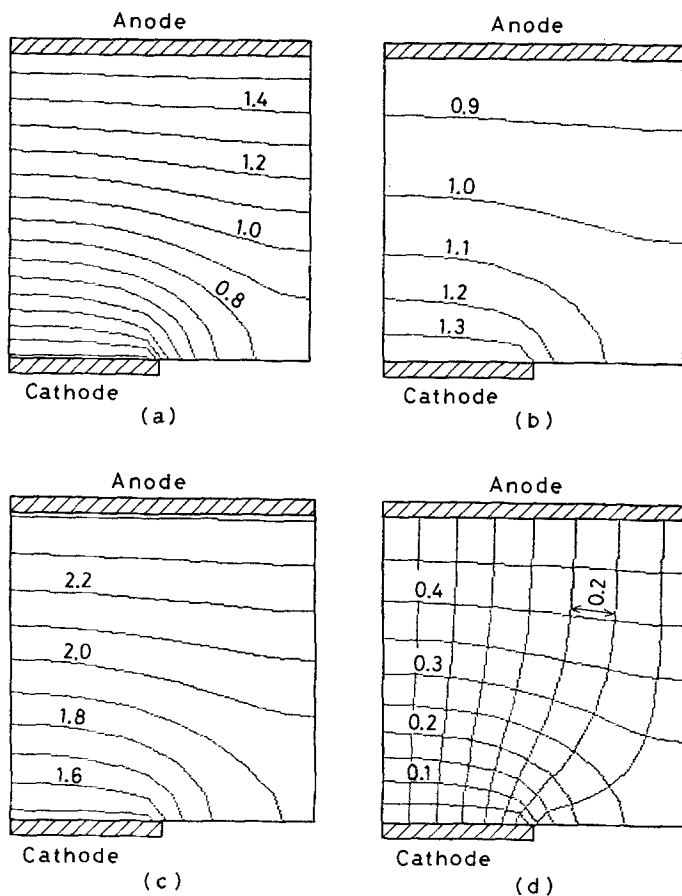


Fig. 5. Concentration distributions of (a) M^+ , (b) S^+ , and (c) A^- , and (d) potential and current distributions in a mixed solution of two electrolytes ($M^+A^- + S^+A^-$). $\Phi(Y=0) = 0$; $\Phi(Y=1) = 0.5$; initial concentrations, $c_{M0} = c_{S0} = c_{A0}/2$. The numbers in figures (a), (b), and (c) indicate the values of C_M , C_S , and C_A , respectively. The numbers on potential lines in figure (d) indicate the values of Φ . The separation between adjacent current lines corresponds to $\Delta\Psi = 0.2$.

$$\begin{aligned} & \left(\frac{(C_M)_{i,1,k} + (C)_{i,0,k}}{2} \right) \left(\frac{(V)_{i,1,k} - (V)_{i,0,k}}{\Delta Y} \right) \\ & + \left(\frac{(C_M)_{i,1,k} - (C)_{i,0,k}}{\Delta Y} \right) \\ & = -I_0 (\exp [(1 - \alpha_c) \{(V_M)_k - (V)_{i,0,k}\}] \\ & - (C)_{i,0,k} \exp [-\alpha_c \{(V_M)_k - (V)_{i,0,k}\}]) \quad (36) \end{aligned}$$

where $(C)_{i,0,k} = (C_M)_{i,0,k} = (C_A)_{i,0,k}$. Two unknowns $(C)_{i,0,k}$ and $(V)_{i,0,k}$ can be calculated from these equations using the Newton-Raphson method. Figure 6 is an example of calculation with $I_0 = 1$ and $\alpha_c = 0.5$. It is noted that equipotential lines cross the electrode surfaces and that current lines do not make right angles to the electrode surfaces.

Bipolarity is sometimes encountered in electrolytic systems and in corrosion cells. Both anodic and cathodic reactions can occur on the bipolar electrode (corroding metal) placed in the potential field in the solution. Conventional methods would require lengthy iterations for the calculation of concentration and potential distributions since boundary conditions at the bipolar metal do not specify either potential or current density. The present method is applicable to such systems. As an example, let us consider a metal plate placed between the anode and the cathode in a simple M^+A^- solution, where dissolution and deposition of metal M take place with Butler-Volmer type kinetics (Equation 31). The geometry of the cell considered is shown in Fig. 7. Boundary conditions at the anode and cathode and at the insulating wall are the

same as described before. Two of the boundary conditions at the bipolar metal are zero flux of A^- and electroneutrality. The other restriction at the bipolar metal is that the total current should be zero:

$$\int i_B dS = 0 \quad (37)$$

where i_B is the current density in the normal direction at the surface, S is the surface area, and integration should be made over the whole surface. The current density i_B is expressed as

$$\begin{aligned} i_B &= -\frac{F^2 D_M}{RT} c_M \frac{\partial \phi}{\partial n} - F D_M \frac{\partial c_M}{\partial n} \quad (38) \\ &= i_0 \left[\exp \left(\frac{(1 - \alpha_c) F (\phi_B - \phi)}{RT} \right) \right. \\ &\quad \left. - \frac{c_M}{c_{M0}} \exp \left(\frac{-\alpha_c F (\phi_B - \phi)}{RT} \right) \right] \quad (39) \end{aligned}$$

where ϕ_B is the potential of the bipolar metal, which must be treated as an additional variable. Now, let us recall the analogy between potential and temperature, and between current density and heat flux. Then we can assume the equation

$$K_B \frac{dv_B}{dt} = - \int i_B dS \quad (40)$$

where K_B is a hypothetical constant (compared to the heat capacity in heat conduction problems). Equation 40 can be compared to the relation between the total heat flux and the rate of change of temperature. If we

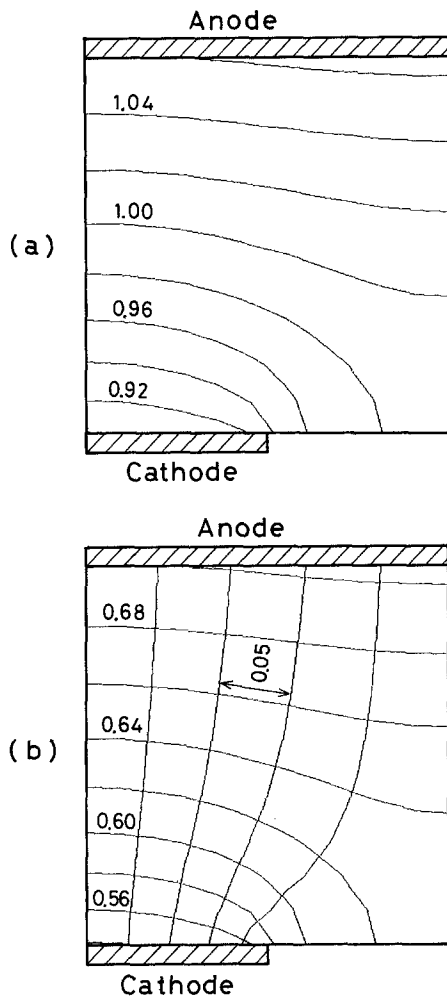


Fig. 6. (a) Concentration distribution of $M^+(A^-)$ and (b) potential and current distributions in a solution of single electrolyte (M^+A^-) with Butler-Volmer kinetics. $\Phi_M(\text{cathode}) = 0$; $\Phi_M(\text{anode}) = 1$; $I_0 = 1$; $\alpha_c = 0.5$; $\Delta\Psi = 0.05$ (see the caption of Fig. 4).

combine Equation 40 with Equations 38 and 39, in which ϕ_B is replaced by $v_B(t)$, and obtain the condition $dv_B(t)/dt = 0$ at $t = \infty$, the value of $v_B(\infty)$ can be regarded as ϕ_B . Equation 40, combined with Equation 38, can be converted to the dimensionless form

$$\frac{dV_B}{d\Theta} = \gamma \int \left(C_M \frac{\partial V}{\partial N} + \frac{\partial C_M}{\partial N} \right) d\sigma \quad (41)$$

where $\sigma = S/\alpha^2$ and $\gamma = F^2 c_{M0} \alpha^3 / K_B RT$. Using forward difference approximation for the derivative $dV_B/d\Theta$ the difference expression for Equation 41 is

$$\begin{aligned} \left(\frac{V_{B,k+1} - V_{B,k}}{\Delta\Theta} \right) &= \gamma \sum_i \left[\left(\frac{(C_M)_{i,1,k} + (C_M)_{i,0,k}}{2} \right) \right. \\ &\times \left(\frac{V_{i,1,k} - V_{i,0,k}}{\Delta Y} \right) \\ &\left. + \left(\frac{(C_M)_{i,1,k} - (C_M)_{i,0,k}}{\Delta Y} \right) \right] \Delta X \quad (42) \end{aligned}$$

The summation should be made over the whole surface of the bipolar metal. Assuming an appropriate value for γ , we can explicitly calculate the V_B value at the time step $k + 1$ from the C , V , and V_B values at the time step k . The calculation procedure for C and

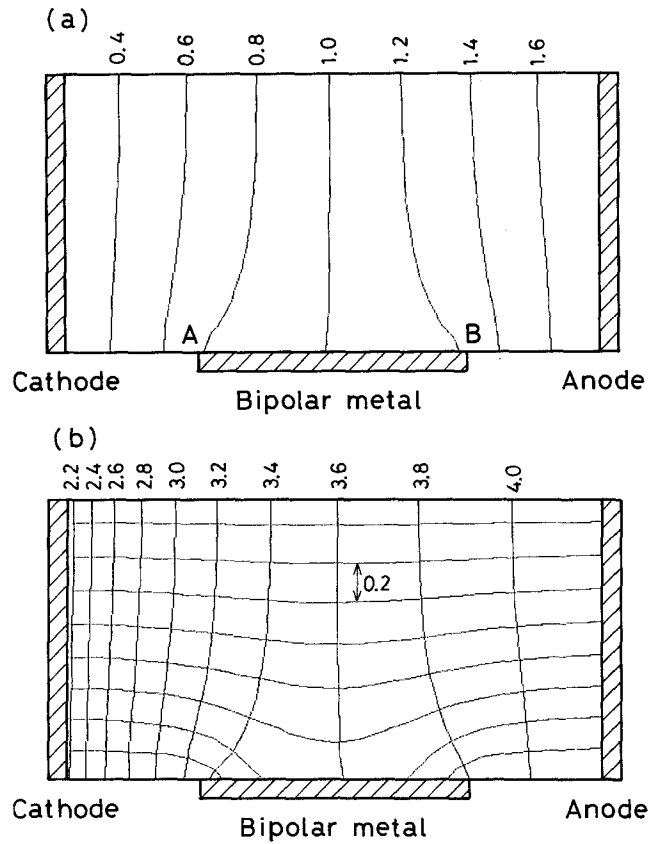


Fig. 7. (a) Concentration distribution of $M^+(A^-)$ and (b) potential and current distributions involving a bipolar metal placed between the anode and cathode. Electrolyte, M^+A^- ; $\Phi_M(\text{cathode}) = 0$; $\Phi_M(\text{anode}) = 5$. The Butler-Volmer kinetics with $I_0 = 10$ and $\alpha_c = 0.5$ is assumed at the anode, cathode, and bipolar metal. $\Delta\Psi = 0.2$ (see the caption of Fig. 4). Dimensionless potential of the bipolar metal, Φ_B , is found to be 3.60.

V is the same as described earlier. Figure 7 shows the calculated results of concentration, potential, and current distributions. Unlike systems with uniform concentrations in the bulk, the low concentration of

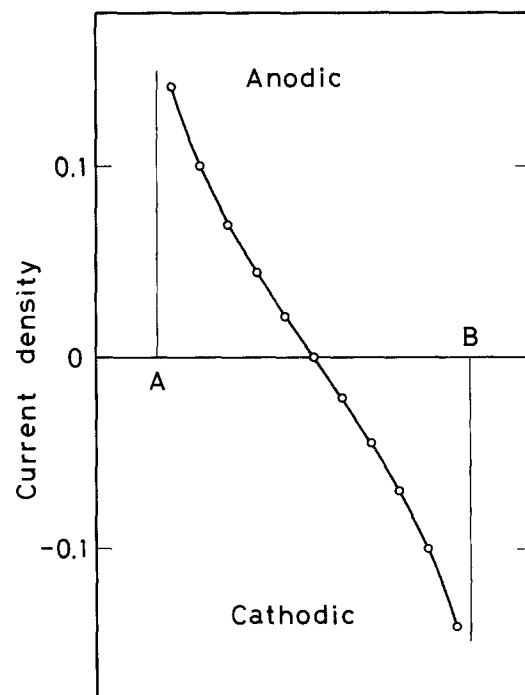


Fig. 8. Current density at the bipolar metal. (See the caption of Fig. 7).

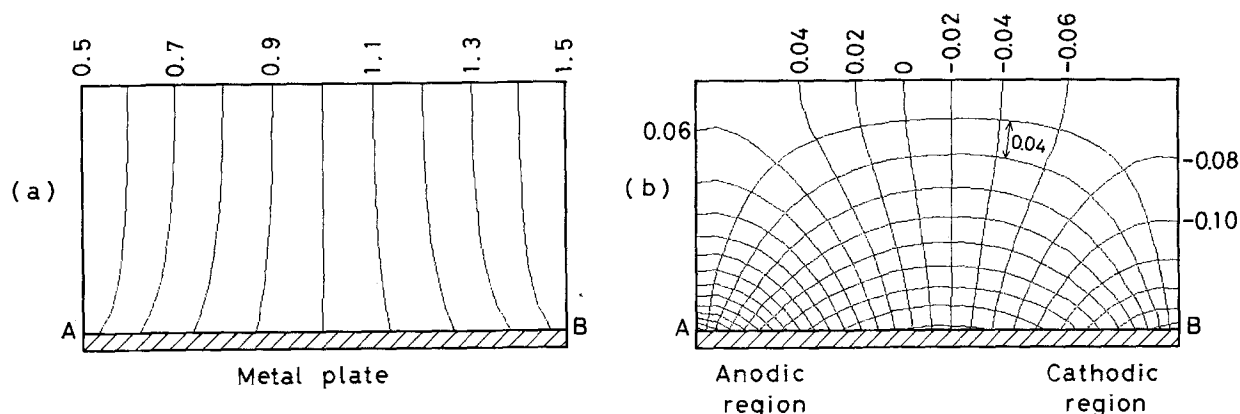


Fig. 9. (a) Concentration distribution of $M^+(A^-)$ and (b) potential and current distributions involving a bipolar metal placed in a concentration gradient of M^+A^- . Electrolyte, M^+A^- ; $C(\text{left}) = 0.5$; $C(\text{right}) = 1.5$; $\Phi_B = 0$. The Butler-Volmer kinetics with $I_0 = 10$ and $\alpha_c = 0.5$ is assumed at the bipolar metal. $\Delta\Psi = 0.04$ (see the caption of Fig. 4).

ionic species near the cathode results in a lower conductivity in the electrolyte, requiring a larger electric field to drive the current, as shown in Fig. 7b. It is apparent that the right-hand part of the bipolar metal becomes cathodic and the left-hand part becomes anodic. Figure 8 shows the current density (dimensionless) on the bipolar electrode as a function of X . It is interesting that the current distribution on the bipolar metal is very symmetric although the potential distribution is asymmetric.

The other example of bipolarity is a kind of local corrosion in which metal M is placed in an M^+A^- solution with a concentration gradient, but without any applied voltage. The geometry of the system considered is shown in Fig. 9. The assumed situation is that the right and left ends are permeable walls and that the M^+A^- concentrations at the two ends are different and kept constant. Dissolution and deposition of metal M take place with Butler-Volmer kinetics (Equation 39). Figure 9 shows an example of calculated distributions of concentration, potential and current. The values of potential, Φ , are expressed with reference to the potential of the bipolar metal,

Φ_B . It is apparent that a local current flows between the anodic and cathodic regions on the metal plate. This is a typical example of metal corrosion due to a concentration cell. Figure 10 shows the current density on the bipolar metal surface. Again, the current distribution is very symmetric. The symmetric behaviour of current distributions observed in Figs 8 and 10 is qualitatively explained by a cancellation of the asymmetric distribution of potential and the asymmetric effect of the M^+ concentration in the kinetics of dissolution and deposition of metal M (Equation 39).

5. Conclusion

A numerical method has been proposed for the calculation of concentration, potential, and current distributions controlled by diffusion and migration of ions. The present method is simple and flexible and has many applications. It is particularly useful for treating bipolar electrodes such as are encountered in local corrosion cells. Its extension to three-dimensional problems will be straightforward; only terms with respect to z need to be added to the relevant equations.

Appendix

One-dimensional distributions of concentrations and potential at steady state can be calculated analytically in an electrolytic solution containing two 1:1 electrolytes (M^+A^- and S^+A^-). The anodic and cathodic reactions are the dissolution and deposition of metal M .

Using dimensionless forms of fluxes, the flux equations for M^+ , S^+ , and A^- are expressed as

$$J_M = -C_M \frac{d\Phi}{dX} - \frac{dC_M}{dX} \quad (\text{A1})$$

$$J_S = \frac{D_S}{D_M} \left(-C_S \frac{d\Phi}{dX} - \frac{dC_S}{dX} \right) \quad (\text{A2})$$

$$J_A = \frac{D_A}{D_M} \left(C_A \frac{d\Phi}{dX} - \frac{dC_A}{dX} \right) \quad (\text{A3})$$

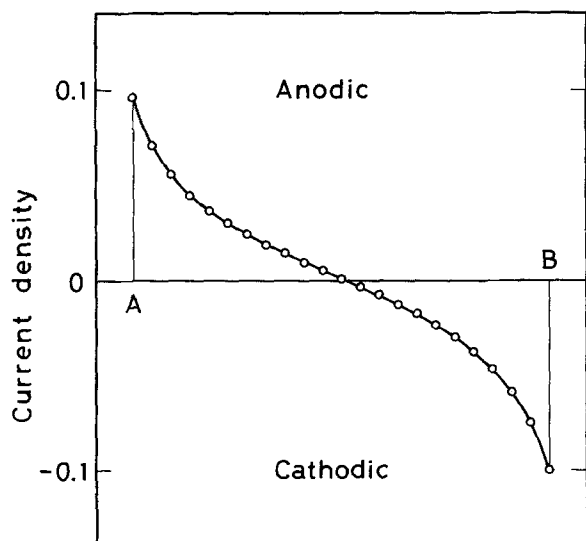


Fig. 10. Current density at the bipolar metal. (See the caption of Fig. 9).

Dimensionless current density is

$$I = J_M + J_S - J_A \quad (\text{A4})$$

Assuming the electroneutrality condition,

$$C_M = C_A - C_S \quad (\text{A5})$$

Since the fluxes of non-electroactive species, S^+ and A^- , are zero everywhere,

$$C_S \frac{d\Phi}{dX} = - \frac{dC_S}{dX} \quad (\text{A6})$$

$$C_A \frac{d\Phi}{dX} = \frac{dC_A}{dX} \quad (\text{A7})$$

Substituting Equation A5 in Equation A1, and using the relations A6 and A7, we obtain

$$J_M = -2 \frac{dC_A}{dX} \quad (\text{A8})$$

Current density is

$$I = J_M = -2 \frac{dC_A}{dX} \quad (\text{A9})$$

At a constant current, integration of Equation A9 yields

$$C_A = C_{A0} - (I/2)(X - 1/2) \quad (\text{A10})$$

where C_{A0} is the dimensionless concentration c_{A0}/c_{M0} . If we define the quantity $k = -I/2C_{A0}$, then

$$C_A = C_{A0} \{1 + k(X - 1/2)\} \quad (\text{A11})$$

Equation A7 can be integrated to give

$$\begin{aligned} \Phi &= \ln C_A + \text{const} \\ &= \ln [C_{A0} \{1 + k(X - 1/2)\}] + \text{const} \end{aligned} \quad (\text{A12})$$

Integration of A6 yields

$$\Phi = -\ln C_S + \text{const} \quad (\text{A13})$$

From A12 and A13, C_S is expressed as

$$\begin{aligned} C_S &= C_{S0} \left(\frac{k}{\ln \{(2+k)/(2-k)\}} \right) \\ &\times \left(\frac{1}{1+k(X-1/2)} \right) \end{aligned} \quad (\text{A14})$$

where C_{S0} is the dimensionless concentration c_{S0}/c_{M0} . Finally the concentration of M^+ is given by

$$\begin{aligned} C_M &= C_A - C_S \\ &= C_{A0} \{1 + k(X - \frac{1}{2})\} \\ &\quad - C_{S0} \left(\frac{k}{\ln \{(2+k)/(2-k)\}} \right) \\ &\quad \times \left(\frac{1}{1+k(X-1/2)} \right) \end{aligned} \quad (\text{A15})$$

For a solution containing single electrolyte M^+A^- ,

$$C_M = C_A = 1 - (I/2)(X - 1/2) \quad (\text{A16})$$

The limiting current density I_{lim} is then calculated from Equation A16 by putting $C_M = 0$ at $X = 0$:

$$I_{lim} = -4 \quad (\text{A17})$$

The solid lines in Fig. 1 were calculated from Equations A16 and A12 with $I = -2$ (half the limiting current density). The solid lines in Fig. 2 were calculated from Equations A11, A12, A14, and A15 with $C_{A0} = 2$, $C_{S0} = 1$, and $I = -2$.

References

- [1] J. Newman, 'Electrochemical Systems', Prentice Hall, Englewood Cliffs, NJ (1973).
- [2] G. A. Prentice and C. W. Tobias, *J. Electrochem. Soc.* **129** (1982) 72.
- [3] N. Ibl, 'Comprehensive Treatise of Electrochemistry', Vol. 6, Plenum Press, New York (1983) pp. 239-315.
- [4] F. Hine, 'Electrode Processes and Electrochemical Engineering', Plenum Press, New York (1985).
- [5] C. Wagner, *J. Electrochem. Soc.* **98** (1951) 116.
- [6] C. W. Tobias and R. Wijnsman, *ibid.* **100** (1953) 459.
- [7] F. Hine, S. Yoshizawa and S. Okada, *ibid.* **103** (1956) 186.
- [8] J. A. Klingert, S. Linn and C. W. Tobias, *Electrochem. Acta* **9** (1964) 297.
- [9] R. Alkire, T. Bergh and R. L. Sani, *J. Electrochem. Soc.* **125** (1978) 1981.
- [10] Y. Nishiki, K. Aoki, K. Tokuda and H. Matsuda, *J. Appl. Electrochem.* **14** (1984) 653.
- [11] H. Kawamoto, *Denki Kagaku* **53** (1985) 98.
- [12] H. Shih and H. W. Pickering, *J. Electrochem. Soc.* **134** (1987) 551.
- [13] E. C. Dimpault-Darcy and R. E. White, *ibid.* **135** (1988) 656.
- [14] K. Asada, F. Hine, S. Yoshizawa and S. Okada, *ibid.* **107** (1960) 242.
- [15] J. Newman, *ibid.* **113** (1966) 1235.
- [16] C. E. Vallet and J. Braunstein, *ibid.* **125** (1978) 1193.
- [17] K. Kontturi and D. J. Schiffrin, *J. Appl. Electrochem.* **19** (1989) 76.
- [18] T. R. Brumleve and R. P. Buck, *J. Electroanal. Chem.* **90** (1978) 1.
- [19] M. M. Menon and U. Landau, *J. Electrochem. Soc.* **134** (1987) 2248.
- [20] Y. Miyazaki, A. Katagiri and S. Yoshizawa, *J. Appl. Electrochem.* **17** (1987) 113.
- [21] Y. Miyazaki, A. Katagiri and S. Yoshizawa, *ibid.* **17** (1987) 877.
- [22] A. Katagiri and Y. Miyazaki, *J. Appl. Electrochem.* **19** (1989) 281.
- [23] A. Katagiri, Extended Abstracts Vol. 2, p. 433, 40th ISE Meeting, 17-22 September 1989, Kyoto, Japan.
- [24] H. S. Carslaw and J. C. Jaeger, 'Conduction of Heat in Solids', Oxford University Press, London (1959).
- [25] N. Ibl, *op. cit.* [3] p. 244.